



HAL
open science

A New Method to Reduce Motion Artifact in Electrocardiogram Based on an Innovative Skin-Electrode Impedance Model

Yajian Gan, Wenceslas Rahajandraibe, Remy Vauche, Blaise Ravelo, Nominoë
Lorriere, Rachid Bouchakour

► **To cite this version:**

Yajian Gan, Wenceslas Rahajandraibe, Remy Vauche, Blaise Ravelo, Nominoë Lorriere, et al..
A New Method to Reduce Motion Artifact in Electrocardiogram Based on an Innovative Skin-
Electrode Impedance Model. *Biomedical Signal Processing and Control*, 2022, 76, pp.103640.
10.1016/j.bspc.2022.103640 . hal-03966572

HAL Id: hal-03966572

<https://hal.science/hal-03966572>

Submitted on 31 Jan 2023

HAL is a multi-disciplinary open access archive for the deposit and dissemination of scientific research documents, whether they are published or not. The documents may come from teaching and research institutions in France or abroad, or from public or private research centers.

L'archive ouverte pluridisciplinaire **HAL**, est destinée au dépôt et à la diffusion de documents scientifiques de niveau recherche, publiés ou non, émanant des établissements d'enseignement et de recherche français ou étrangers, des laboratoires publics ou privés.

A New Method to Reduce Motion Artifact in Electrocardiogram Based on an Innovative Skin-Electrode Impedance Model

Yajian GAN¹, Wenceslas RAHAJANDRAIBE¹, Remy VAUCHE¹, Blaise RAVELO², Nominoë LORRIERE¹ and Rachid BOUCHAKOUR³,

¹ Aix Marseille Univ, Université de Toulon, CNRS, IM2NP, Marseille, France

² Nanjing University of Information Science & Technology (NUIST), Nanjing, Jiangsu 210044, China

³ WitMonki, 565 Avenue du Prado, 13008 Marseille

Corresponding author: Yajian GAN, yajian.gan@im2np.fr

Abstract

The electrocardiogram (ECG) is sensitive to human body motions when it is measured with dry metal electrodes. A common hypothesis in previous literature dealing with these subjects postulate that this is due to the skin-electrode impedance variability. This paper aims to verify this hypothesis by investigating the origin of the noise in the ECG signal and finding suitable solutions to reduce this disturbance. For this reason, experiments are proposed here to explore the relationship between the skin-electrode impedance and the ECG for several motions. Results demonstrate that the noise due to human body motions in ECG equally comes from the electrochemical equilibrium break of the reduction-oxidation reaction at the skin-electrode interface. Moreover, it has been shown that motions lead to sweat thickness variations and equally to skin-electrodes capacitance variations. To model this phenomenon, an electrical model based on a variable capacitor is introduced. Finally, a significant noise reduction solution based on the monitoring of this capacitor is proposed.

Keywords: ECG monitoring, impedance measurement, skin-electrode interface model, noise analysis, motion artifact

1. Introduction

An electrocardiogram (ECG) signal can be measured with wet or dry electrodes. Conventional disposable wet electrodes such as Ag/AgCl electrodes, the type most used for medical applications, provide excellent signal quality thanks to the embedded electrolyte gel which helps to create a good electrical connection between the electrode and human tissue. However, they are limited to single-use and can sometimes lead to allergic contact dermatitis [1]. To avoid these problems, many consumer cardiac monitoring systems often use dry electrodes without electrolyte gel. [2-3]. Unfortunately, the measured signal quality, in terms of signal-to-noise ratio (SNR), of these dry electrodes used in consumer products, is often inferior to that of an ECG obtained with a medical-grade device. In fact, the unstable connection between dry electrodes and human tissue in turn means that these electrodes can be particularly sensitive to motion during the ECG. [4-5].

According to the work of Vargas Lunas [6], the skin-electrode impedance can directly reflect the changes in the skin-electrode contact surface and the ECG quality. Thus, for wet electrodes which are attached to the human tissues, the gel guarantees the stability of the skin-electrode impedance even if a motion occurs. On the contrary, for dry electrodes which do not include gel, the variation of the skin-electrode impedance leads to a noisy and distorted ECG.

Taji B. has measured in [7] the variations of the skin-electrode impedance according to the pressure applied on the electrode. When the pressure increases, impedance decreases, resulting in a higher quality ECG measurement. To monitor these variations during ECG measurement, an impedance measurement circuit has been proposed in [8].

This paper aims to verify the relationship between the skin-electrode impedance and the artifacts of motion in the ECG signal by further investigating the origin of the noise. It also proposes a method to reduce motion artifacts.

Section II presents the test bench setup used during these experiments. It also reviews the measured skin-electrode impedance and the ECG signal quality for different specific motions and constraints. Section III proposes an evolution for the commonly used electrical model of the skin-electrode impedance. This optimized model takes into consideration both the observed impedance variations and the motion artifact noise in the ECG signal during the experiments in section II. In section IV, a simple ECG signal correction method based on the monitoring of the skin-electrode capacitance is proposed. Finally, Section V gives the conclusions of this study.

2. Material and methods

2.1. *Introduction of the test bench*

To start, the person who is operating as the test subject is asked to sit down in front of the test equipment and firmly press each thumb to the left and right dry electrodes on the test pad which is hypothesized to be sensitive to motion. Simultaneously, wet electrodes are attached to the inside of each wrist as shown in Fig. 1. A two-channel ADInstruments PowerLab 35 series instrument is then used to collect the ECG signals coming from both the-dry thumb electrodes and the wet electrodes attached to the inside of the wrists. Because this study evaluates the change in ECG signal based on impedance fluctuations of that ECG signal, the electrodes are connected to an Agilent E4980A LCR meter that gives detailed impedance data in the frequency range [20Hz – 2MHz]. The LCR meter is in turn controlled with a LabVIEW-developed program. This control program then extracts the impedance modulus values Z and their associated argument values θ for eight frequencies (60 Hz, 80 Hz, 125 Hz, 200 Hz, 250 Hz, 375 Hz, 500 Hz, 1000 Hz). These frequencies were chosen as they represent key points of interest showing the plot curve trend. Points above 1000Hz are moving toward denser static residual resistance. Frequency points below 60Hz plot the other half of a typical RC circuit impedance spectroscopy graph image. Because the data acquisition time increment is supposed to be less than the time increment of the impedance fluctuation itself (caused by the movement of the test subject), the measurements of frequency less than 60Hz can be ignored. Lastly, a Tektronix AFG1022 instrument is used to send a trigger signal that is used to synchronize the above-mentioned Agilent E4980A LCR meter to the PowerLab 35 series ADInstruments.

Fig. 2 shows the ECG signals when the test subject is completely stationary. In this stationary case, the plot of the dry electrode ECG shows very little variation with respect to the plot of the wet electrode ECG as demonstrated by only slight differences between the two plots amplitude and offsets. After applying a bandpass filter between 1 and 20 Hz, with a transition bandwidth of 8 Hz, the two signal plots show an even closer coincidence. So, the use of this filter for this initial calibration test showing the close coincidence of the two ECG plots allows us to deduce that any other dissimilarities between the wet electrode and dry electrode ECG signals be caused by the motion of the test subject or other constraints.

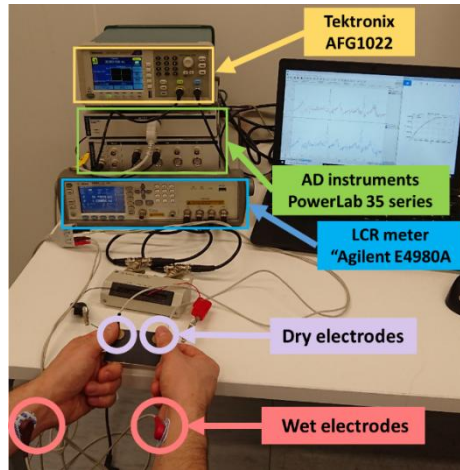


Fig. 1. ECG and skin-electrode impedance measurement

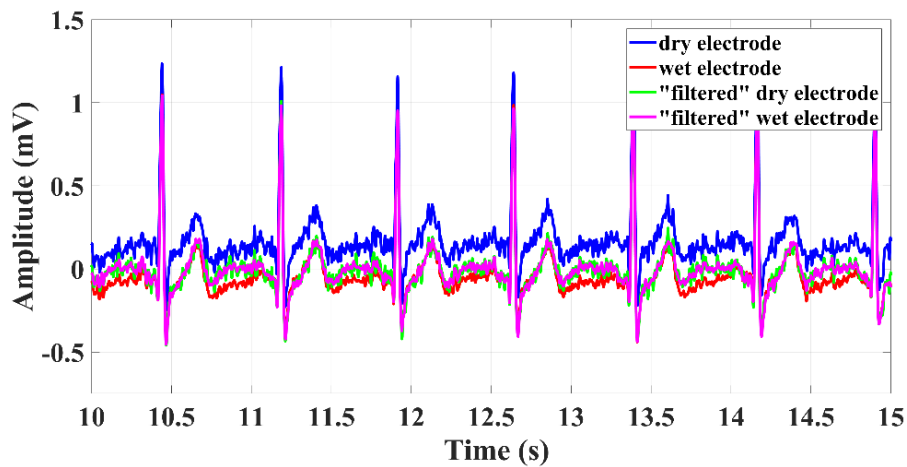


Fig. 2. ECG from wet and dry electrodes during “stay still” test

To guarantee the reliability of impedance measurements, the stationary subject experiment, from onwards referred to as the “stay still” experiment is repeated every day for one week (52 measurements per day). For each frequency, the measured impedance constitutes a points cloud. A plot of these mean values as well as the standard deviation of the impedance (Nyquist plot: imaginary part of the complex conjugate impedance versus the real part of the complex impedance) is shown in Fig. 3 for each frequency. In the case of a statistic measurement, the mean data points define the parameters of the electrical equivalent circuit made by the skin-electrode contact and the dispersion of the points cloud defines the type A uncertainty [9] for this impedance measurement system. In other words, from a statistical point of view, they can be used to define the measurement uncertainty of the proposed experiment. Nevertheless, this “stay still” impedance is as expected relatively stable and will be used as a reference to identify motions impact on the skin-electrode impedance.

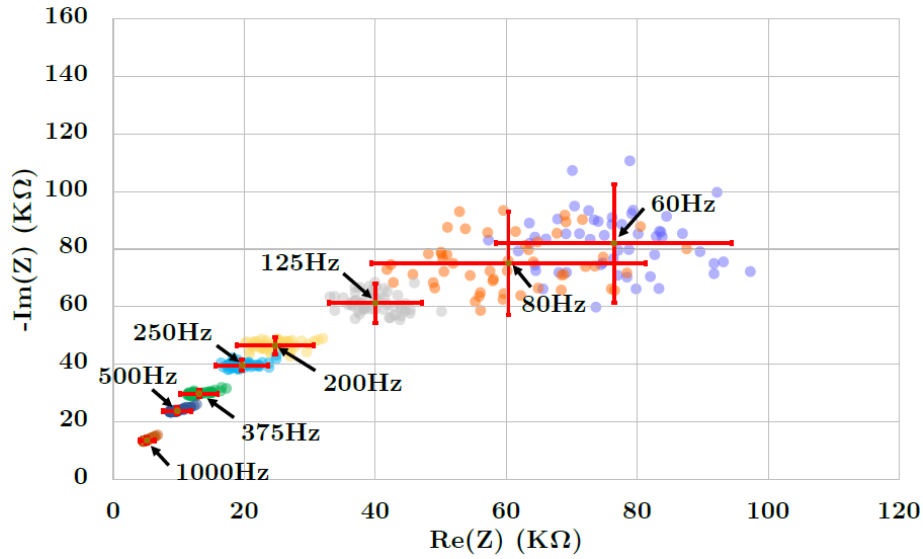


Fig. 3. Nyquist plot of the impedance for “stay still” experiment

Thus, the values of the standard deviation and the mean value in "stay still" mode have been set as the standard uncertainty, or confidence interval, for the real and imaginary sections of the measure impedance for each frequency. Statistically significant impedance variations for different motions can be identified by the overlapping of these confident intervals. [10]. For example, if the standard deviation and the mean value of the skin-electrode impedance obtained during a particular motion are not within or close to these ranges, this particular motion will be considered as a motion that disturbs the skin-electrode impedance.

2.2. Correlation between the recorded ECG signal and the measured skin-electrodes impedance

2.2.1. Definition of four elementary variables associated to motions

Residual signals left in the data from various motions, or data motion artifacts, contains many parameters to analyze. It is proposed to separate the motions that can cause these data artifacts into four individual categories, listed as the variables “muscle activation”, “friction”, “pressure level” and “contact area”. These four basic motion variables, their impact on ECG signals and the subsequent protocols to measure them will be discussed next.

“Muscle activation”: this test is collected motion data when the test subject, while still firmly placing each thumb on the dry electrode pad, or pinching the pads, is allowed to move their hands in a motion following a virtual square of approximately 20cmx30cm with a speed between $0.3 \text{ m}\cdot\text{s}^{-1}$ and $0.4 \text{ m}\cdot\text{s}^{-1}$ while attempting to not vary the pressure on the pads or surface area covered on the pads with the thumbs.

“Friction”: this test is to collect motion data when the test subject is allowed to move the thumbs over the contact pads with an approximate speed of $0.01 \text{ m}\cdot\text{s}^{-1}$ (verified with the assistance of an accelerometer) while attempting to not change the contact surface area nor the pressure on the contact pads.

“Pressure level”: this test is to collect motion data when the test subject is kept in the “Stationary Subject” state as a background reference. However, with this test, an external system is put into place that can add varying levels of pressure onto the thumbs which are in turn already firmly pressed to the contact pads. The three different pressure levels to be evaluated will be: light (2N), medium (5N), and high (10N).

“Contact area”: this test is similar to “stay still” reference measurement. However, the contact surface

between the thumbs and electrodes will be set by covering a part of the electrodes surface using an insulating material as shown in fig.4. The four tested contact surfaces are 25%, 50%, 75%, and 100% of the electrode surface.

To determine if these four variables have an impact on the impedance and induce noise on the ECG signal, results will be compared to “stay still” reference measurement previously presented.

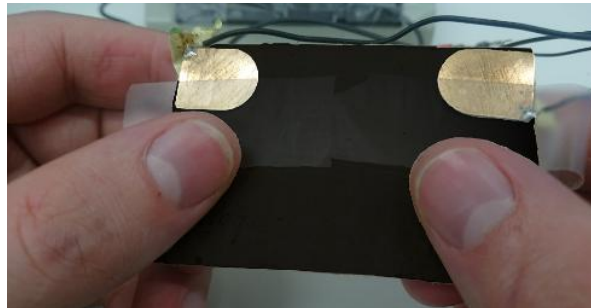


Fig. 4. Example for a 50% contact area

2.2.2. Results for “Muscles activation”

Fig. 5 shows the Nyquist plot [11] of the skin-electrodes’ impedance obtained for “Muscles activation”. For each frequency, the points distribution is similar to those obtained during “stay still” experiment. This amplitude of error bars indicates that the contraction and the relaxation of the muscle did not influence the impedance.

The ECG recorded during the test is shown in Fig. 6. Both wet and dry electrode signal channels show the same high-frequency noise which is caused by the surface electric potential generated by muscle cells [12] when the tester moves his hands. The associated voltage of this electric potential, called electromyogram (EMG), is typically in the range of hundreds of microvolts and spans the frequency range of 5 - 100 Hz [13]. Because the frequency range of the ECG and EMG can overlap, we applied a filter of 1 - 20 Hz to reduce the EMG signal while allowing the ECG signal to remain clear. However, regardless of this filtering of the EGM filtering or not, the EGC signal from the wet and dry electrodes almost coincide. By comparing the data of this ECG test with that of the “stay still” experiment (Fig.2), it is possible to conclude that the “muscles activation” test shows an influence on the ECG signal even if the impedance appears to stay stable.

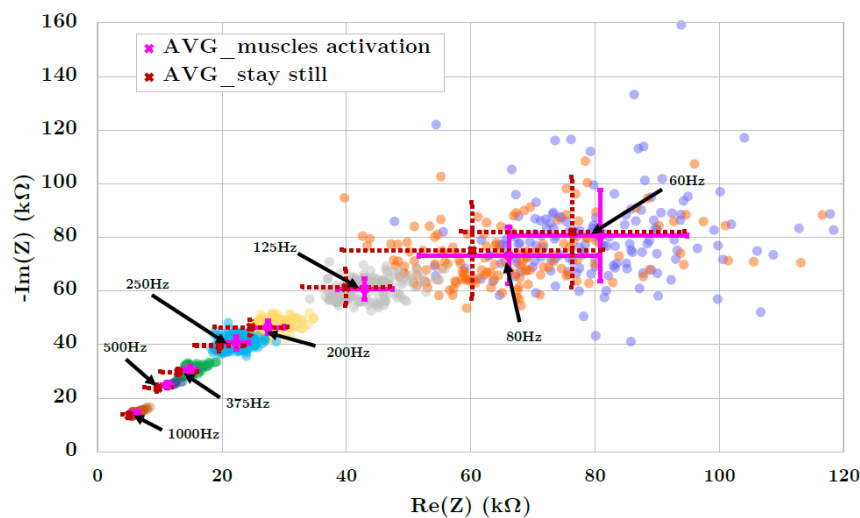


Fig. 5. Nyquist plot of the measured impedances for “muscles activation”.

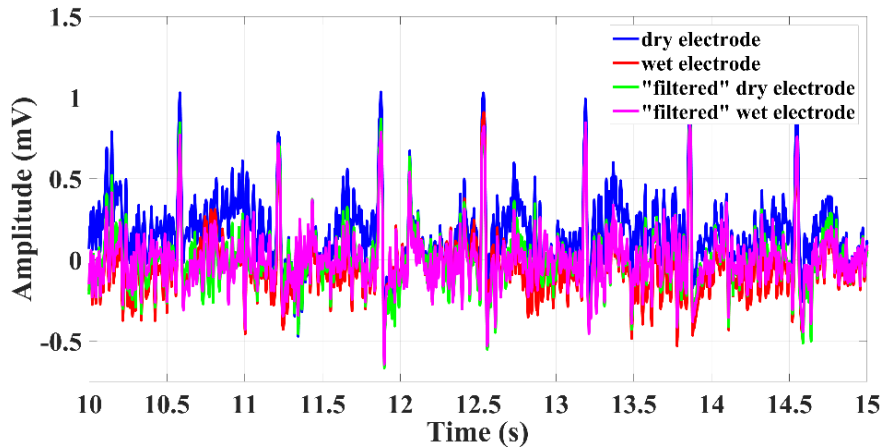


Fig. 6. ECG from the two channels during “muscles activation” test.

2.2.3. Results for “friction”

Fig. 7 shows the Nyquist plot of the skin-electrode impedances for the “friction” test. It shows that the average impedance has changed though it must be noted that this could be caused by inconsistencies in how the test subject holds the electrodes while performing the test. Nevertheless, the standard deviation shows that “friction” does not have a significant influence on the measured impedance.

Fig.8 however shows a high amplitude noise on the ECG measured with the dry electrodes. Even if a filter is used, the quality of the signal is not much improved when compared to the ECG recording using wet electrodes. This in turn demonstrates that the “friction” has a significant influence on the ECG signal.

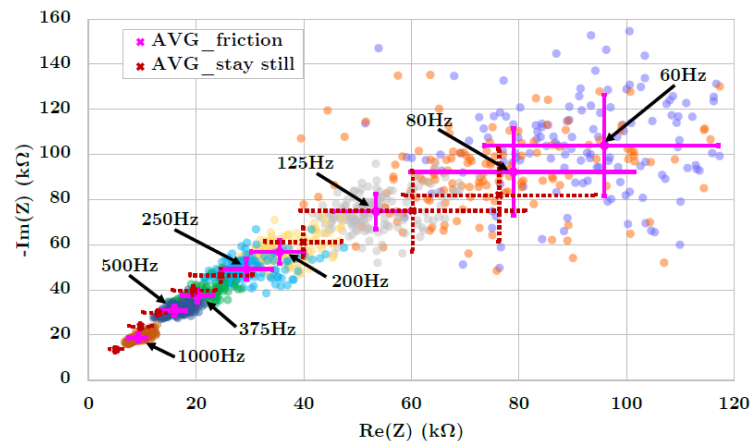


Fig.7. Nyquist plot of the measured impedances for “friction” experiment.

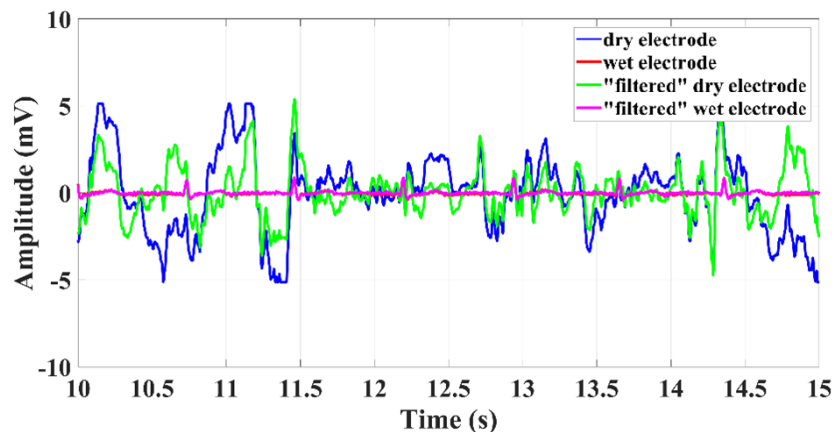


Fig. 8. ECG from the two channels during “friction” test.

2.2.4. Results for “pressure level”

In Fig. 9, the average and standard deviation of the impedance has been computed for each frequency tested and at every pressure level. The distribution cloud points show similarity to the distribution cloud points obtained during “stay still” experiment. This in turn implies that the application of different pressures levels on the dry electrode pads surface does not have a substantial effect on the impedance.

In Fig. 10, the ECGs levels from the dry electrode channel and the wet electrode channel while applying medium pressure to the dry electrode pads, are shown to be close. In addition, the two signals almost coincide after applying the filter. Thus, the “pressure level” test does not appear to have much influence on the ECG signal and test.

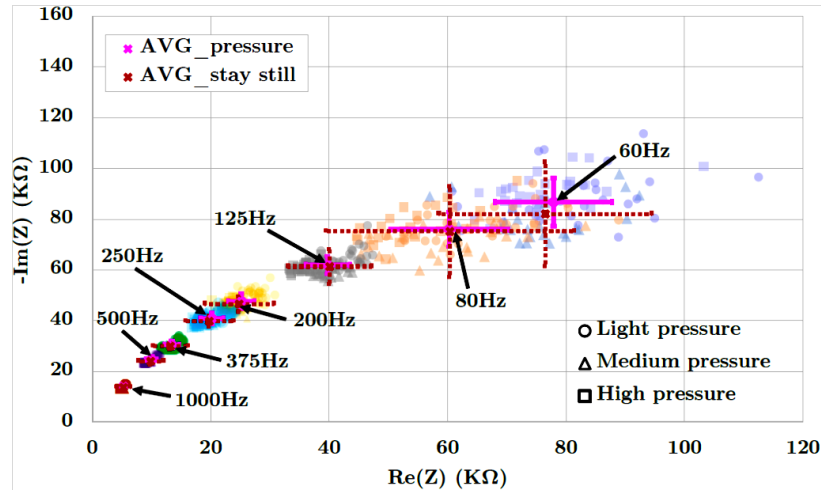


Fig. 9. Nyquist plot of the measured impedances for “pressure level” experiment.

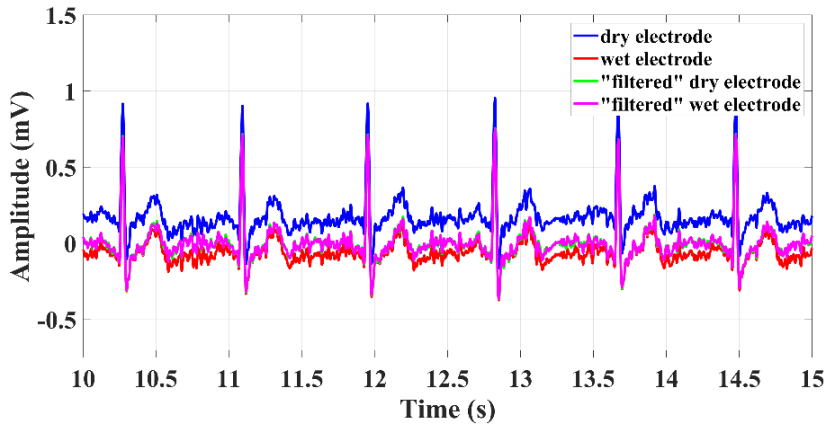


Fig. 10. ECG from the two channels during “Medium pressure level” test.

2.2.5. Results for “contact area”

In Fig. 11, the different point shapes represent the impedance for each given percentage of contact surface tested. Compared to the impedance values obtained during the “stay still” experiment, both real and imaginary parts of the impedance are widely distributed. Moreover, the points distribution for both “25% surface” and “50% surface” are very irregularly distributed for all tested frequencies. However, impedance values for both “75% surface and “100% surface” show a much closer correlation to each other, though a rather significant difference can be observed for the standard deviation values. It is also perhaps more relevant to plot each points distribution clouds instead of plotting a standard deviation cross near the average impedance. From these observations, it is possible to say that the higher percent contact areas demonstrate a more stable impedance. Conversely, the data from the ECG signals from both the wet and dry electrodes indicate that “contact surface” does not significantly influence the ECG results.

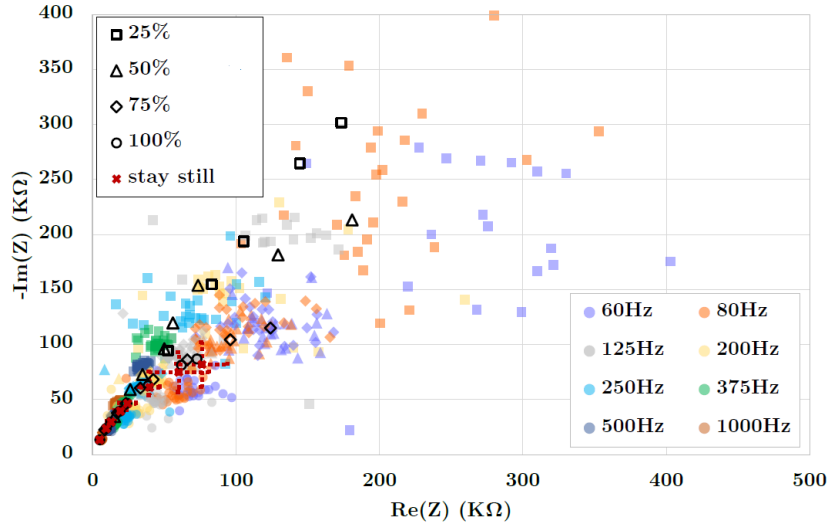


Fig. 11. Nyquist plot of the measured impedances for “contact area” experiment.

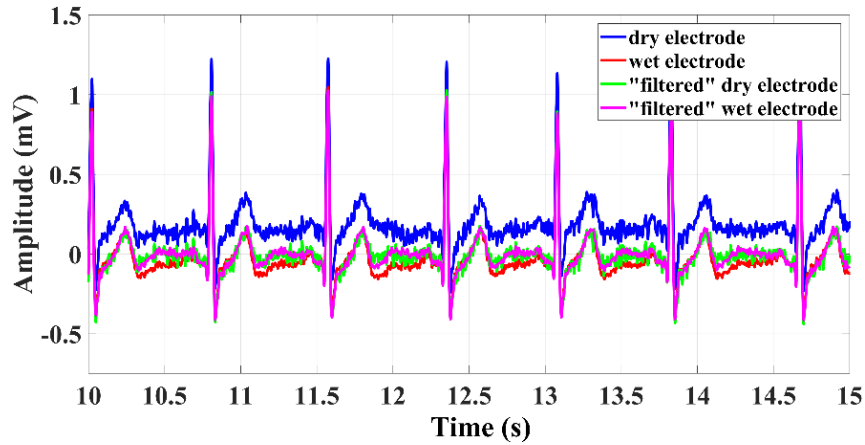


Fig. 12. ECG from the two channels during “contact area” test (25%).

3. Modeling and analysis

3.1. Equivalent electrical circuit model for skin-electrode impedance

When electrodes are attached to the skin, the different skin layers, up to an attached electrode, can be modeled electrically as shown in Fig. 13. An equivalent electrical model on the first order is used to model the dry electrode-skin impedance [14-17] and introduced the voltage source term $E_{el/s}$. Indeed, the oxidation-reduction reactions [18] between the electrodes (metal) and the sweat (electrolyte) induce ion exchange as shown in Fig. 14 which, by the end of the reaction, reaches electrochemical equilibrium. At this moment, a fixed electric field appears which is called the half-cell potential E_{hc} , which in turn is represented by the term $E_{el/s}$ as shown in Fig.13. This first-order model also introduces the terms R_e and C_e which serve to help model the electrical behavior of the epidermis and the term R_d which helps model the resistance of the skin’s dermis layer.

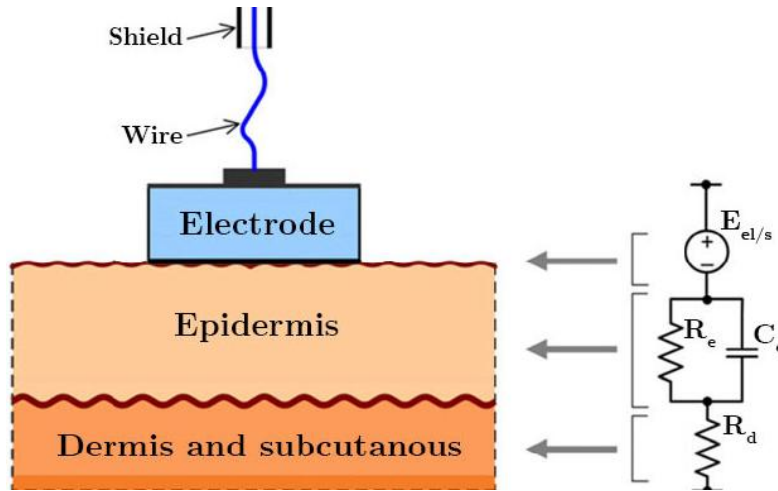


Fig. 13. Skin-electrode interface layers and first order electrical equivalent model.

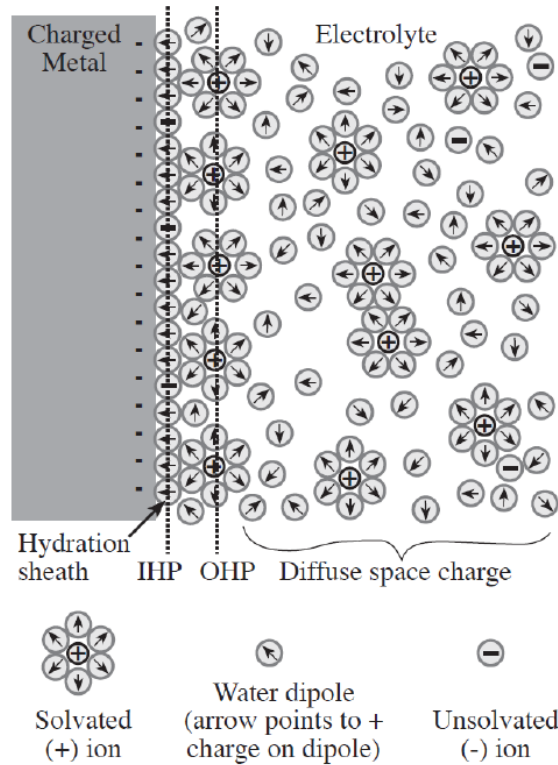


Fig. 14. Electrochemical equilibrium of the skin-electrode interface [19-20].

However, more realistic models which have been proposed to model the skin-electrode interface, generally use the Constant Phase Element (CPE) term instead of the C_e capacitor term. This term comes into play when considering the sweat layer in between the skin-electrode contact. Sweat in contact with the metal of the electrode can be considered as an electrolytic fluid that has a specific electrical behavior due to the thin thickness of this sweat layer in between the electrode-skin interface. This specific electrical behavior can be modeled with the help of the CPE term and the impedance is then defined as [21] the following:

$$Z_{CPE}(\omega) = \frac{1}{Q(j\omega)^n}$$

where:

- $\omega = 2\pi f$ is the angular frequency [$\text{rad}\cdot\text{s}^{-1}$],

- Q is the capacitive effect of the CPE [$\Omega^{-1} \cdot s^n$],
- n is a constant ($0 \leq n \leq 1$) which represents the inhomogeneities of the interface surface.

Thus, Fig. 15 shows the equivalent electrical circuit seen between the electrodes involving the CPE when thumbs pinch the electrodes for the “stay still” configuration.

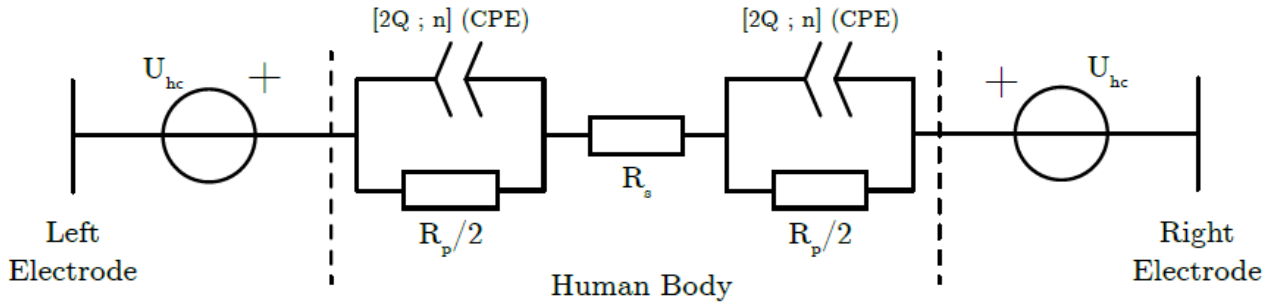


Fig. 15. Equivalent electrical circuit seen between the electrodes for “Stay still” configuration.

The results of the experiments show that during the “Friction” test, a significant disturbance in ECG signal can be detected while at the same time no impedance variation has been measured. It is also possible to consider that any disturbance of the ECG signal may be coming from variations of the half-cell potential U_{hc} . Indeed, with any relative movement between the thumbs and dry electrodes, the electrochemical equilibrium is continuously disturbed during the movement. In this case, the half-cell potential can no longer be considered as a constant, and it is more appropriate to model the half-cell potential induced by this charge distribution as a variable generated voltage. Thus, according to [22] and as shown in Fig. 16, the half-cell charge distribution and capacitance variations can also be modeled as a variable capacitor that varies according to the charge’s distribution in the electrolyte layer.

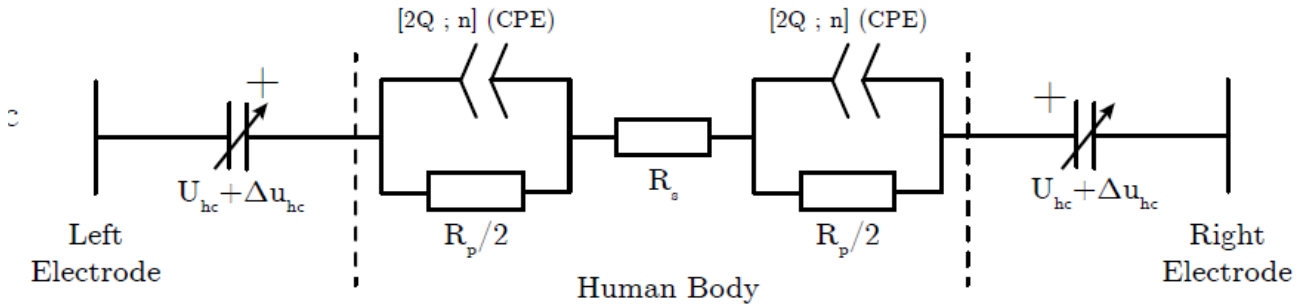


Fig. 16. Equivalent electrical circuit seen between the electrodes for the configurations associated to motions.

3.2. Experimental ECG signal and the measured skin-electrodes impedance data analysis

Fig. 17 presents the impedance standard deviation (STD) for each elementary variable associated with the various motion tests. It appears that “pressure level”, “muscle activation” and “friction” do not have a measurable impact on the skin-electrode impedance variability. However, the skin-electrode impedance is mainly influenced by the change of the contact surface area and this influence is found to be so high that it is more relevant to plot the data points cloud instead of the standard deviation crosses around the average impedance, as previously discussed.

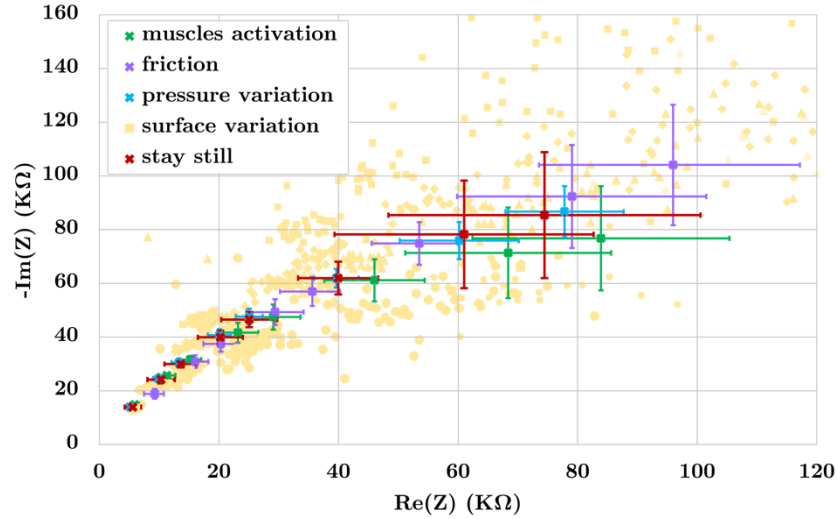


Fig. 17. STD of the impedance for each elementary motion.

The coefficient of variation (CV) of measured impedance, which is defined as the ratio of the standard deviation σ to the mean μ of measured impedance for any given motion, is used in Fig. 18 to highlight the change of impedance values (for which “move” in Fig. 18 corresponds to “muscle activation”). Indeed, compared with STD, CV eliminates any scaling effects and is more appropriately used here since the absolute value of the skin-electrode impedance values can vary significantly depending on the conducted test and the tester. It can also be seen in Fig. 18 that the higher values of CV are obtained for the lower tested contact surface areas. Thus, the percentage of contact surface area significantly affects the skin-electrode impedance. From a general point of view, the lower the contact surface area is, the higher the variability of the skin-electrode impedance.

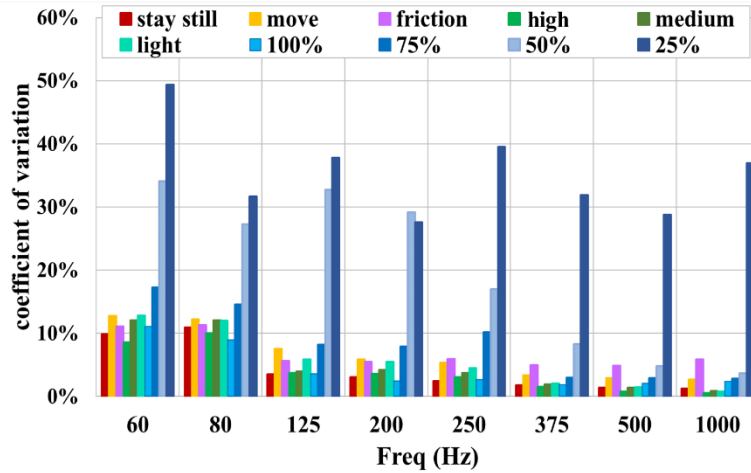


Fig. 18. Coefficient of variation of the impedance for each elementary variables associated to motions (light, medium, and large correspond to the three tested three “pressure level” and 25%, 50%, 75%, and 100% correspond to the four tested “contact area”).

To further evaluate the influence of each of the four elementary motion variables (“friction”, “muscle activation”, “pressure level” and “contact area”, along with the “stay still” variable) effects on the ECG signal, three “rates” are plotted versus the tested “motions” as shown in Fig. 19. The first “rate” used is the correlation coefficient (listed as “Correlation” on the graph) between the ECG measured with dry electrodes and the reference ECG measured with wet electrodes. The second and the third “rates” used are, respectively, the sensitivity (SEN) term and the threat score (TS) term. These in turn are defined by the terms true positive (TP), false positive (FP), true negative (TN), and false negative (FN) defined as follows [23]:

$$\text{SEN} = \text{TP} / (\text{TP} + \text{FN})$$

$$TS = TP / (TP + FP + FN)$$

These variables are then applied to the resultant data obtained when using arguably the most used benchmark heartbeat detection algorithm by Pan & Tompkins [24] on ECG signals.

As shown in Fig. 19, “pressure level” and “contact area” have similar rates to the “stay still” measurement. Thus, these two elementary variables have little influence on the ECG signal. However, the rates obtained for “muscles activation” and “friction” shows that “muscles activation” has a medium influence on the ECG signal (about 75% of heartbeats are detected) whereas “friction” has a high influence on the ECG signal (less than 15% of heartbeats are detected). Indeed, “muscles activation” brings light interference noise to ECG signals whereas “friction” introduces much more significant noise to ECG signals.

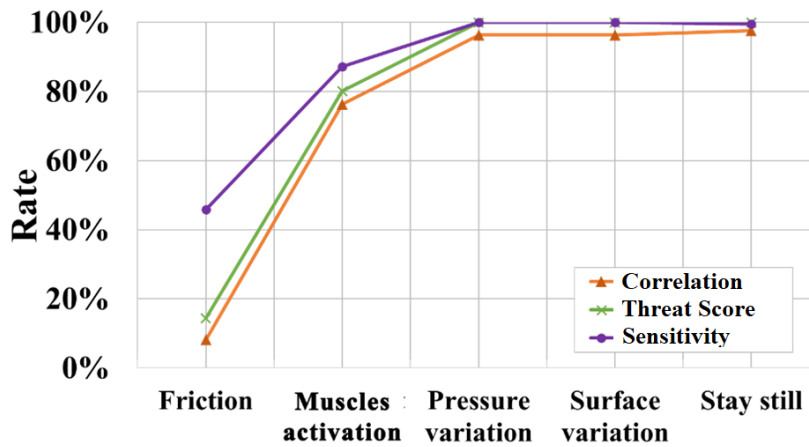


Fig. 19. Rates to evaluate the influence of elementary motions on ECG distortion.

3.3. Relationship between the skin-electrode impedance and the ECG signal

The four elementary motion variables have different impacts on the variation of the recorded impedance and the ECG signals. Skin-electrode impedance is mainly affected by “contact area” whereas ECG signal is predominately affected by the “muscles activation” and “friction” tests. Table 1 summarizes these influences.

Elementary variable	Influence on the impedance variations	Influence on ECG
"Muscles activation"	No	Yes
"Friction"	No	Yes
"Pressure level"	No	No
"Contact area"	Yes	No

Table 1. Influence on the impedance and ECG of each elementary variable associated to motions.

The leading cause of noise in the ECG signal during the “muscles activation” test is the EMG which distorts the ECG in both amplitude and frequency whereas, during the “friction” test, the interference of the ECG signal mainly comes from the accumulation and release of charge from when the thumbs rub on the surface of the electrodes. To help eliminate the interferences caused by “friction”, some researchers have proposed a new kind of silicon-based dry electrode for measuring biological signals. It uses microneedle arrays to penetrate the stratum corneum which reduces skin impedance variations [25]. For the “muscles activation” interferences, filtering methods can be used to filter out the interferences of EMG signal from the ECG. While the impedance is neither sensitive to the change of the charges on the surface, nor the EMG.

However, the size of the “contact area” influences the skin-electrode impedance signal while the ECG signal remains clean since the electrolyte interface [26] is fixed during the proposed experiment and stays in a balanced state with the fixed contact surface. Thus, this experimental result is perfectly explained by the new electrical equivalent skin-electrode model proposed in Fig. 16.

4. Result and discussion

4.1. Validation of the optimized equivalent electrical circuit model

In a specific test to verify the skin-electrode electrical equivalent model, the pressure applied on the dry electrode pads by the test subject’s thumbs was dynamically changed by the tester during the experiment as described next. Between 10 s and 12.5 s, the pressure was changed slowly; between 12.5 s and 14 s, the pressure was changed quickly; after 14 s, the pressure was again changed slowly. The associated recorded ECG signals are shown in Fig. 20, and it can be shown that for the dry electrodes the ECG baseline follows these variations in pressure. Moreover, it can be noted that the ECG baseline decreases when the pressure is decreased, and it increases when the pressure is increased. Then, when pressure variations occur slowly enough regarding the filter being used, ECG baseline variations are correctly filtered. However, when pressure variations occur too quickly, the ECG signal becomes too distorted to be interpreted.

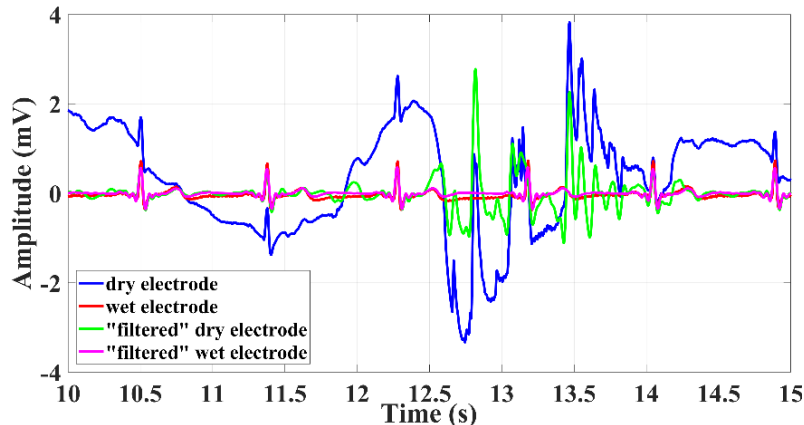


Fig. 20. Influence of pressure variations on the ECG signal measured with dry electrodes.

The same pressure variation tests were conducted with wet electrodes and as shown in Fig. 21 similar results were recorded. As can be seen in Fig. 22, it can be noted that during the test with the wet electrodes, the pressure applied on the electrodes has been high enough to induce deformation of the plastic and the gel, exceeding its reversible viscoelasticity strain capacities. Meanwhile, the amplitude of the fluctuations is only 2.4 times greater than the reference ECG signal for the wet electrode test, whereas it was 7 times greater than the reference ECG signal for the previous dry electrode test. Compared to dry electrodes where the only fluids layer is the body fluid that acts as the electrolyte, such as sweat, wet electrodes contain a thicker conductive gel, which makes them more resistant to pressure variations since the gel helps to compensate for the fast morphology and thickness variations of the electrolyte layer. Thus, the main difference between the wet electrodes and dry electrode tests comes from the conductive layer in the wet electrode, which is thicker, with a firmer surface tension thanks to its conductive gel. The constant surface tension of the conductive gel on the wet electrode also helps to compensate for any pressure variation applied on the contact surface.

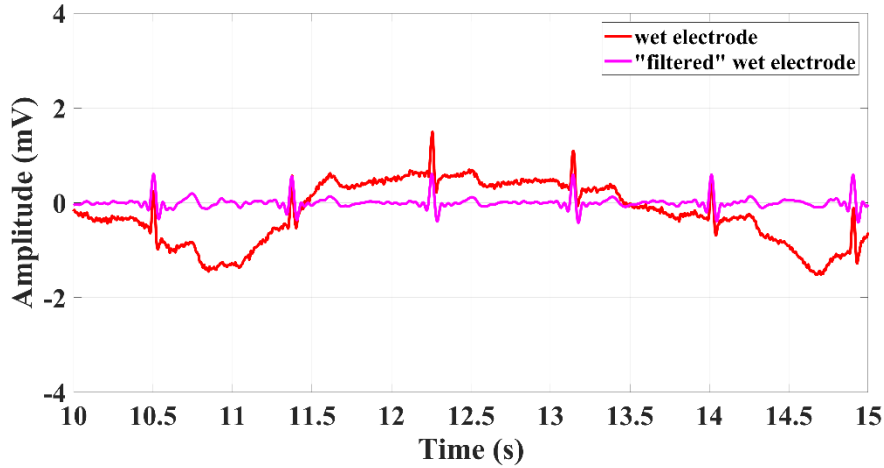


Fig. 21. Influence of pressure variations on the ECG signal measured with wet electrodes.



Fig. 22. Initial (left) and final (right) state of wet electrodes used during pressure variation tests.

4.2. Filtering of motion artifacts in the ECG signal

As shown earlier, dynamic pressure variations on the electrodes can directly cause voltage fluctuations in recorded ECG signals. Indeed, with a variation in the thickness of the sweat layer (which acts as a conductive layer between the skin and the electrodes), the skin-electrode electrochemical equilibrium can be disrupted and broken. The process to try to rebalance this signal can itself induce noise on ECG signal recording. Variations of the sweat thickness can also cause variations in the capacitance (C_s) between the electrodes and are the main source of the parasitic voltage. Thus, a large part of the parasitic voltage could be predicted by monitoring the thickness variations of the sweat and C_s capacitance variations. Fig. 23 shows an ECG recording synchronized with the real-time measurement of C_s and demonstrates this concept. For this reason, it is proposed here to compensate for parasitic noises in ECG signaling by measuring continuously the C_s capacitance with the help of an LCR meter. It is, however, challenging to find the appropriate transfer functions which could enable the implementation of an active feedback loop to eliminate real-time noise interferences caused by the subject's motion movement.

In this paper, it is assumed that the noise voltage and capacitance have a linear relation between them. Using linear regression, the parasitic voltage (y) can be predicted by the C_s value in F (x) as follows:

$$y=0.0037x-0.0832$$

Fig. 24 shows the predicted voltage noise while using this simple linear model. It proves that the predicted voltage has the same order of magnitude as the measured voltage and follows the same trend. To measure the similarity between the predicted voltage and the measured voltage, the mean square error (MSE) as defined in [27] is used and is equal to 1.9×10^{-4} .

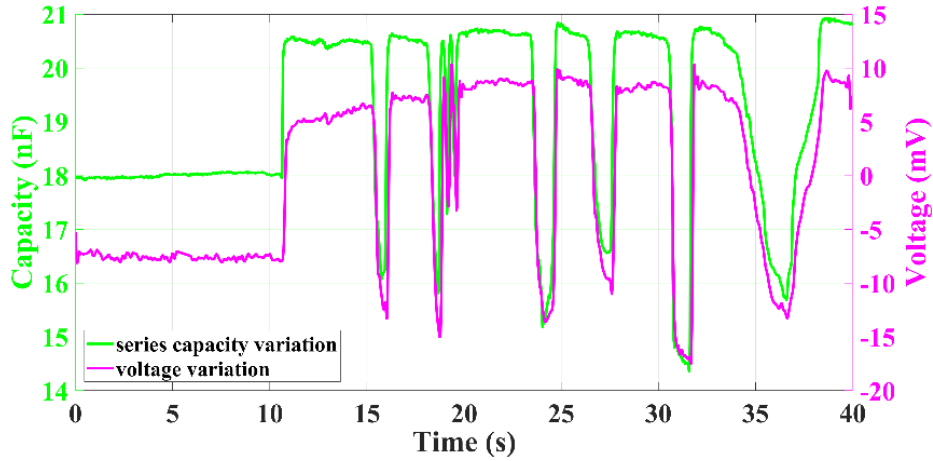


Fig. 23. Recorded ECG signal synchronized with the measured C_s capacitance.

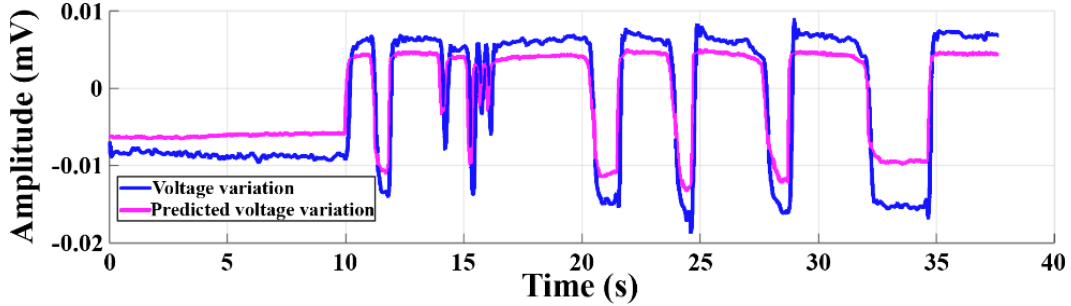


Fig. 24. Prediction of the noise voltage using the proposed simple linear model.

Fig. 25 shows the ECG signal collected with the dry electrodes and corrected using the proposed method. The signal collected using the wet electrodes is also shown as a reference. The ECG signal collected by the dry electrodes in blue shows significant disturbance due to various motions, whereas the corrected ECG signal in green matches more closely the ECG signal collected by the wet electrodes. Thus, the parasitic voltage caused by motions has been satisfactorily eliminated since the shape of the electrical impulsion of the heart (called the QRS complex) [13] has been saved, thanks to the C_s measurement that has been used to predict the parasitic voltage.

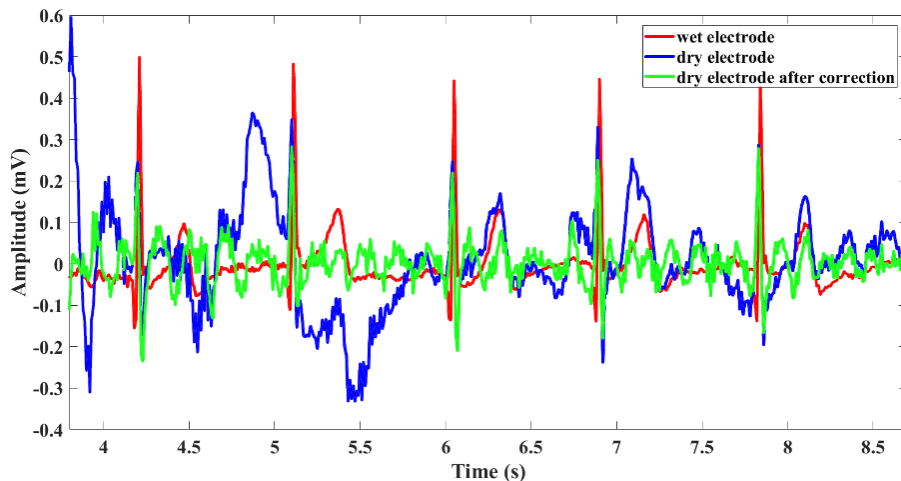


Fig. 25. Result of the ECG motion artifact correction

5. Conclusion

This paper aims to explore the sources of motion noise and then reduce this motion noise in ECG signals. For this reason, several experiments have been conducted that demonstrate that ECG signal instability is not, as proposed in many references' materials, only caused by the variability of the skin-

electrode impedance. For example, induced friction can lead to a break in the electrochemical equilibrium of the reduction-oxidation reaction at the skin-electrode interface and induce noise in the ECG signal. This can be modeled by a variable voltage source. Nevertheless, it has been shown that pressure variations on the electrodes can lead to variations in thickness in the sweat layer which in turn leads to skin-electrodes impedance variations and skin-electrodes capacitance variations. To model this phenomenon, the variable voltage source has been replaced by a variable capacitance in the electrical model introduced in this paper. Next, it has been experimentally demonstrated that variations in the skin-electrodes capacitance signal very closely follow the noise from various motions during an ECG test. The result of this work has produced a solution to eliminate the observed noise in ECG testing. Indeed, the parasitic voltage has been successfully predicted by monitoring the capacitance value seen between the electrodes with a simple linear model. Future work must now focus on other methods, such as lasso regression or machine learning algorithm, to improve the accuracy of the predicted parasitic voltage from the monitored skin-electrodes capacitance value.

References

- [1] N. Meziane, J. Webster, M. Attari, et al., “Dry electrodes for electrocardiography”, *Physiological Measurement*, 34, no., R47–R69, 2013. doi: 10.1088/0967-3334/34/9/R47.
- [2] U. G. okhan Guven, Hakan Gürka, “Biometric identification using fingertip electrocardiogram signals,” *Signal, Image Video Process.*, pp. 1–8, 2018. doi:10.1016/j.patrec.2018.03.028 (Article in. Press).
- [3] Y. Gan, R. Vauche, J.-F. Pons, W. Rahajandraibe “Dry Electrode Materials for Electrocardiographic Monitoring”, 25th IEEE International Conference on Electronics Circuits and Systems (ICECS), Bordeaux, France, 2018. doi: 10.1109/ICECS.2018.8617992.
- [4] A. Searle and L. Kirkup, “A direct comparison of wet, dry and insulating bioelectric recording electrodes,” *Physiol. Meas.*, vol. 21, no. 2, pp. 271–283, 2000. doi: 10.1088/0967-3334/21/2/307.
- [5] Y. M. Chi, T. P. Jung, and G. Cauwenberghs, “Dry-contact and noncontact biopotential electrodes: Methodological review,” *IEEE Rev. Biomed. Eng.*, vol. 3, pp. 106–119, 2010. doi: 10.1109/RBME.2010.2084078
- [6] J. L. Vargas Luna, M. Krenn, J. A. Cortés Ramírez, and W. Mayr, “Dynamic Impedance Model of the Skin-Electrode Interface for Transcutaneous Electrical Stimulation,” *PLoS One*, vol. 10, no. 5, pp. 1–15, 2015. doi:10.1371/journal.pone.0125609
- [7] B. Taji, S. Shirmohammadi, and V. Groza, “Measuring skin-electrode impedance variation of conductive textile electrodes under pressure”, *Proceeding: IEEE International Instrumentation and Measurement Technology Conference*, no., pp. 1–6, 2014. doi: 10.1109/I2MTC.2014.6860909.
- [8] S. Kim, R. Yazicioglu, T. Torfs, et al., “A 2.4 μ a continuous-time electrode-skin impedance measurement circuit for motion artifact monitoring in ecg acquisition systems”, *Proceeding: 2010 Symposium on VLSI Circuits*, no., 2010. doi: 10.1109/VLSIC.2010.5560290.
- [9] M. E. Payton, A. E. Miller, and W. R. Raun, “Testing statistical hypotheses using standard error bars and confidence intervals,” *Commun. Soil Sci. Plant Anal.*, vol. 31, no. 5–6, pp. 547–551, 2000. doi:10.1080/00103620009370458.
- [10] N. Schenker and J. Gentleman, “On judging the significance of differences by examining the overlap between confidence intervals”, *The American Statistician*, 55, no., pp. 182–186, 2001. doi: 10.1198/000313001317097960.
- [11] G. W. Walter, “A review of impedance plot methods used for corrosion performance analysis of painted metals,” *Corros. Sci.*, vol. 26, no. 9, pp. 681–703, 1986. doi: 10.1016/0010-938X(86)90033-8.
- [12] H. Liang, Z. Lin, and F. Yin, “Removal of ECG contamination from diaphragmatic EMG by nonlinear filtering,” *Nonlinear Anal. Theory, Methods Appl.*, vol. 63, no. 5–7, pp. 745–753, 2005. doi: 10.1016/j.na.2004.09.018.
- [13] G. Bortolan, I. Christov, I. Simova and I. Dotsinsky, “Noise processing in exercise ECG stress test for the

analysis and the clinical characterization of QRS and T wave alternans”, *Biomedical Signal Processing and Control*, no. 18, pp. 378–385, 2015. doi: 10.1016/j.bspc.2015.02.003.

[14] M. Neuman, *The Biomedical Engineering Handbook: Second Edition*, Biopotential electrodes, J. Bronzino, Ed. CRC Press, 2000.

[15] C. Assambo, A. Baba, R. Dozio, et al., “Determination of the parameters of the skinelectrode impedance model for ecg measurement”, *Proceeding: 6th WSEAS International Conference on Electronics, Hardware, Wireless and Optical Communications*, no., pp. 90–95, 2007. doi: 10.5555/1355643.1355660.

[16] B. Taji, S. Shirmohammadi, and V. Groza, “Measuring skin-electrode impedance variation of conductive textile electrodes under pressure”, *Proceeding: IEEE International Instrumentation and Measurement Technology Conference*, no., pp. 1–6, 2014. doi:10.1109/I2MTC.2014.6860909.

[17] J. Luna, M. Krenn, J. Ramírez, et al., “Dynamic impedance model of the skinelectrode interface for transcutaneous electrical stimulation”, *PLoS ONE*, 10, no., pp. 1–15, 2015. doi: 10.1371/journal.pone.0125609.

[18] Y.D. Gamburg, and G. Zangari, “Theory and Practice of Metal Electrodeposition”, Springer, 2011. doi: 10.1007/978-1-4419-9669-5.

[19] J. Bockris and A. Reddy, *Modern Electrochemistry*. Plenum, 1973, vol. 2. doi: 10.1007/978-1-4613-4560-2.

[20] A. Borkholder, “Cell based biosensors using microelectrodes”, PhD thesis, Stanford University, 1998.

[21] E. McAdams, A. Lackermeier, J. McLaughlin, et al., “The linear and non-linear electrical properties of the electrode-electrolyte interface”, *Biosensors & Bioelectronics*, 10, no., pp. 67–74, 1995. doi: 10.1016/0956-5663(95)96795-Z.

[22] H. Wang and L. Pilon, “Accurate simulations of electric double layer capacitance of ultramicroelectrodes”, *The Journal of Physical Chemistry C*, 115, no., pp. 16711-16719, 2011. doi: 10.1021/jp204498e.

[23] Q. Qin, J. Li, Y. Yue, et al., “An adaptive and time-efficient ecg r-peak detection algorithm”, *Journal of Healthcare Engineering*, 2017, no., pp. 1–14, 2017. doi: 10.1155/2017/5980541.

[24] J. Pan and W. Tompkins, “A real-time qrs detection algorithm”, *IEEE Transactions on Biomedical Engineering*, BME-32, no., pp. 230–236, 3 1985. doi: 10.1109/TBME.1985.325532.

[25] Y. Wang, W. Pei, K. Guo, et al., “Dry electrode for the measurement of biopotential signals”, *Science China*, 54, no., pp. 2435–2442, 2011. doi: 10.1007/s11432-011-4354-0.

[26] David A. Borkholder, “Cell Based Biosensors Using,” A Diss. Submitt. to Dep. Electr. Eng. committe Grad. Stud. stanford Univ. Partial fulfillment Requir. degree Dr. Philos., 1998.

[27] D. Wallach and B. Goffinet, “Mean squared error of prediction as a criterion for evaluating and comparing system models”, *Ecological Modelling*, 44, no., pp. 299–306, 3-4 1989. doi: 10.1016/0304-3800(89)90035-5.